PHYSICS AND CHEMISTRY OF SOLID STATE
V. 27, No. 2 (2026) pp. 372-381
Section: Physics

DOI: 10.15330/pcss.27.2.372-381

Vasyl Stefanyk Carpathian National University

ФІЗИКА І ХІМІЯ ТВЕРДОГО ТІЛА
Т. 27, № 2 (2026) С. 372-381
Фізико-математичні науки

PACS: 72.80.-r, 78.66.Jg

ISSN 1729-4428 (Print)
ISSN 2309-8589 (Online)

V.M. Kryshenik[1], I.M. Voynarovych[1], A.I. Pogodin[2], M.J. Filep[1,3], V.V. Halyan[4], M.M. Pop[2], V.V. Rubish[1], T.Y. Babuka[2], A.V.Gomonnai[1]

Electrical conductivity and optical properties of annealed $(As_2S_3)_{1-x}Ag_x$ alloys

[1]*Institute of Electron Physics, Nat. Acad. Sci. Ukr., Uzhhorod, Ukraine, kryshenik@gmail.com;*
[2]*Uzhhorod National University, Uzhhorod, Ukraine;*
[3]*Ferenc Rákóczi II Transcarpathian Hungarian University, Berehovo, Ukraine;*
[4]*Lesia Ukrainka Volyn National University, Lutsk, Ukraine*

The paper presents the results of study of physical properties of synthesised by melt quenching and thermally annealed $(As_2S_3)_{1-x}Ag_x$ ($0.04 \le x \le 0.40$) alloys depending on the silver content. Temperature dependences of the electric conductivity of the alloys under study measured in the 293 to 413 K range in the direct and alternate current (DC and AC) modes showed that the dominating mechanism is thermally activated charge-carrier hopping mediated by delocalised states in the tails close to the energy bandgap boundaries and localised states close to the Fermi level. Thermal activation energy for the alloy ionic conductivity estimated from the Arrhenius plots increases with silver content. For bulk $(As_2S_3)_{1-x}Ag_x$ samples with $x = 0.30$ and 0.40 AC electric conductivity studies revealed the presence of two components in the charge transfer mechanism due to specific features of their inhomogeneous structure. The effect of the increasing Ag content in the $(As_2S_3)_{1-x}Ag_x$ alloys on the optical absorption edge, energy bandgap, and refractive index dispersion in the visible and infrared ranges is studied. For thermally annealed alloys with high Ag content the optical bandgap shrinks and the refractive index increases.

Keywords: amorphous chalcogenides, DC and AC electric conductivity, optical absorption edge, refractive index.

Received 23 November2025; Accepted 03May2026, Published 29 June 2026.

Introduction

Within recent decades, intense studies of semiconducting chalcogenide glasses and alloys produced a vast array of data on their unique structural, electronic, and optical properties [1, 2]. These materials are promising as media for modern photonics and optoelectronics, capable for information recording and transformation, infrared and nonlinear optics, electronic memristors, thermoelectric generators, electrochemical sensors and displays [3–9]. Semiconducting chalcogenide alloys of As–S systems with metals introduced in their structure attract researchers due to the dominating ionic type of conductivity, efficient stimulated diffusion of dopant atoms, polarity-dependent electric switching with memory effect. This makes them promising for practical applications in solid-state ionics [10, 11].

As_2S_3 chalcogenide glasses are generally known to possess quite low electric conductivity which restricts their electrotechnical applications. Doping such glasses with transition metals like Ag or Cu intensely improves their electric transport-related properties [11]. With increasing metal content, their ionic conductivity can essentially increase from 10^{-14} S cm^{-1} to 10^{-5} S cm^{-1} [12]. Earlier chalcogenide alloys in a rather broad range of silver content, from several ppm up to 30–35 at. % Ag were studied [11, 13]. In these investigations two experimental techniques were successfully combined: electrical studies with separation of residual electronic conductivity of the base matrix and much more pronounced ionic component, and studies of optical properties of chalcogenide alloys in the visible and near infrared ranges [11, 14]. Contrary to selenide glassy

system with introduced silver, for the $(As_2S_3)_{1-x}Ag_x$ alloys the effect of the residual electronic conductivity is, as a rule, too small. As a rule, at low Ag doping level (not exceeding several units ppm), $(As_2S_3)_{1-x}Ag_x$ glasses are electrical insulators. Above the percolation threshold in the Ag doping level (~8 at. %) abrupt changes in ionic transport were observed, namely a stepwise transition from the residual electronic to the dominating ionic conductivity type [12]. A noticeable (by several orders of magnitude) increase of the electric conductivity parameter σ with an accompanying change of the cationic diffusion activation energy parameter is a direct reflection of such percolation transition [11, 15]. Results of distinct changes in the structure of doped glasses, in particular, due to possible presence of submicrometer-type inhomogeneities (phase separation in the as-prepared glass) were revealed in optical studies [16–21].

In the present work we studied how the content of Ag in the $(As_2S_3)_{1-x}Ag_x$ alloys and subsequent thermal treatment of the samples affect their electrical and optical properties.

I. Experimental

Bulk glassy $(As_2S_3)_{1-x}Ag_x$ ($0.04 \le x \le 0.40$) alloys were prepared by one-temperature synthesis. Appropriate amounts of presynthesised As_2S_3 glass and colloidal Ag were loaded in quartz ampoules evacuated to 10^{-2} Pa and heated to 870 K. At this temperature the melt was kept at constant stirring for 4 h and rapidly quenched in air.

Binary As_2S_3 glass was presynthesised from elemental components (purity 99.999%) in the stoichiometric ratio in a quartz ampoule evacuated to 10^{-2} Pa which was constantly rotated around its axis. The ampoule was heated to 920 K and quenched in cold water.

The procedure of thermal annealing of the $(As_2S_3)_{1-x}Ag_x$ alloys was performed in evacuated molten quartz ampoules at 523 K for 1 and 4 h.

X-ray studies of the $(As_2S_3)_{1-x}Ag_x$ alloys were carried out using a Proto Manufacturing Ltd diffractometer equipped with a DECTRIS MYTHEN2R 1D hybrid photon detector. The measurements were performed in Bragg-Brentano configuration using a Cu K_α X-ray source.

For electrical measurements the alloys were shaped in plane-parallel plates with polished surfaces with approximate dimensions 5×4×0.9 mm. Electric contacts were provided by two gold electrodes and the measurements were performed using a specially designed holder in the temperature range 293–440 K. For DC measurements a B7-30 electrometer was used in a standard electric circuit.

Direct current (DC) electric conductivity σ_{DC} was determined as

$$\sigma_{DC} = \frac{d \cdot I_{DC}}{U_{DC} \cdot S} \qquad (1)$$

where I_{DC} is the measured current, U_{DC} is the applied voltage, and d is the thickness of the sample with a cross-section S.

Alternate current (AC) electric measurements for $(As_2S_3)_{1-x}Ag_x$ alloys were carried out using electrochemical impedance spectroscopy (EIS) [22] in the frequency range 1×10^1 – 3×10^5Hz in the temperature interval 293–383 K using a high-precision LCR-meter AT 2818. The AC amplitude was 500 mV. In this case samples under investigation could be considered an equivalent of a capacitor C_p with a parallel connected resistor R_p.

The measurements were performed by a two-electrode method with gold contacts applied by vacuum thermal evaporation. The electric conductivity was calculated from the value of resistance R as $\sigma = d/(RS)$ where S is the electrode surface and d is the distance between the electrodes.

Optical transmission spectra of the As_2S_3:Ag alloys in the range of 400–1100 nm were measured using a UV-1700 spectrometer (Macylab Instrument). Refractive index dispersion of $(As_2S_3)_{1-x}Ag_x$ glasses in the spectral interval of 440–1000 nm was studied using a Horiba Smart SE spectral ellipsometer. The experimentally obtained spectra were analysed using DeltaPsi2 software.

An IRAffinity-1S (Shimadzu) Fourier spectrometer was used for the studies of infrared transmission spectra in the range of 2–22 μm (450–5000 cm^{-1}).

II. Results and discussion

X-ray diffraction (XRD) patterns of as-prepared as well as thermally annealed $(As_2S_3)_{1-x}Ag_x$ (x = 0.2, 0.3, and 0.4) glassy alloys are shown in Fig. 1. XRD measurements show that the as-prepared (unannealed) samples possess amorphous structure without any evidence of the presence of crystalline phases. For high silver content level in the alloy (x = 0.4) in the diffractograms of the as-prepared sample weak features were revealed which, with certain caution, can be related to crystalline inclusions. Detailed study of the XRD patterns and corresponding analysis performed earlier [19] enabled us to assume presence of inclusions of As_4S_4 crystalline phase (alacranite) in the unannealed $(As_2S_3)_{0.6}Ag_{0.4}$ alloy.

Meanwhile, thermal annealing of the sample with x = 0.3 in an evacuated quartz ampoule at the temperature 523 K for 1 and 4 h resulted in the formation of another crystalline phase in the glass matrix (Fig. 1), evidenced by distinct features in the diffractograms at 28°, 32,5°, and 46.4°. We compared the diffraction patterns with the reference data for probable crystalline phases of $AgAsS_2$ (smithite [23] and trechmannite [24]), Ag_3AsS_3 (proustite [25] and xanthoconite [26]) as well as for Ag_2S (acanthite [27]).

Comparison of the diffraction patterns for the thermally annealed $(As_2S_3)_{0.7}Ag_{0.3}$ alloys with the known data for the above crystals enabled us to assume that main crystalline phases emerging in the course of the sample annealing are smithite and (less probable) proustite. The presence of the former is supported by the effect of phase separation, well known for the Ag–As–S glass system [19, 28, 29]. In particular, for synthesised amorphous $(As_2S_3)_{1-x}Ag_x$ alloys with Ag content exceeding 20 at. %, the fraction of silver-enriched non-crystalline phase close to $AgAsS_2$ increased [16, 19].

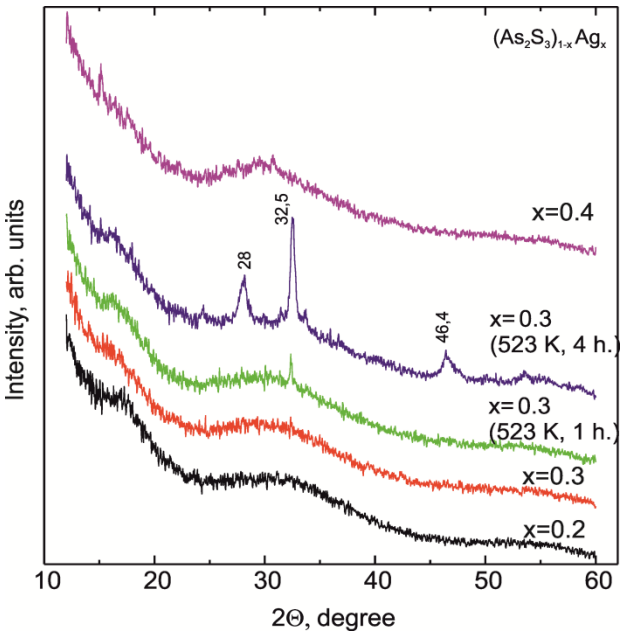

Fig. 1. XRD patterns of as-prepared as well as thermally annealed $(As_2S_3)_{1-x}Ag_x$ alloys.

We performed an experimental study of temperature and frequency dependences of the electric properties of $(As_2S_3)_{1-x}Ag_x$ alloys with various Ag content to elucidate a possible mechanism of charge transfer in these materials.

The results of the DC electric conductivity measurements for the as-prepared $(As_2S_3)_{1-x}Ag_x$ alloys with various Ag content are shown in Fig. 2. We revealed that in this case the electric conductivity value σ_{DC} in the alloys with relatively small silver content $(0.04 \le x \le 0.20)$ exponentially increases with temperature and this increase is described by a typical Arrhenius dependence

$$\sigma_{DC} = \sigma_0 \cdot exp\left(-\frac{\Delta E_\sigma}{k_B T}\right) \qquad (2)$$

where σ_0 is the pre-exponential factor, k_B is the Boltzmann constant, ΔE_σ is the DC conductivity activation energy, T is temperature.

Such linear functional dependence $\ln(\sigma_{DC}) = f(1/T)$ for $(As_2S_3)_{1-x}Ag_x$ alloys with $0.04 \le x \le 0.2$ is generally typical for semiconducting chalcogenide glasses, for which for which the electric conductivity is thermally activated with participation of delocalised energy states in the energy gap close to its boundaries (density-of-states tails). Appearance of the latter is mostly caused by structural disordering, structural defects of various type, and presence of impurity inclusions [30]. A sharp increase of the ionic conductivity for $(As_2S_3)_{1-x}Ag_x$ glasses at $x > 0.20$ is directly related to the increase of the density of energy states in the charge-carrier limited mobility gap [31] with overcoming the above mentioned percolation transition at a certain level of silver doping. Evidently, introduction of additional amount of Ag atoms will cause an increase of charge-carrier concentration due to the appearance of new energy states and will affect the Fermi level position [32].

For bulk samples with $x \ge 0.3$ the electric conductivity σ_{DC} at room temperature reaches $\sim 10^{-7}$ S cm^{-1}; meanwhile, at a noticeable increase of temperature a deviation from the Arrhenius-type dependence is possible (See Fig. 2).

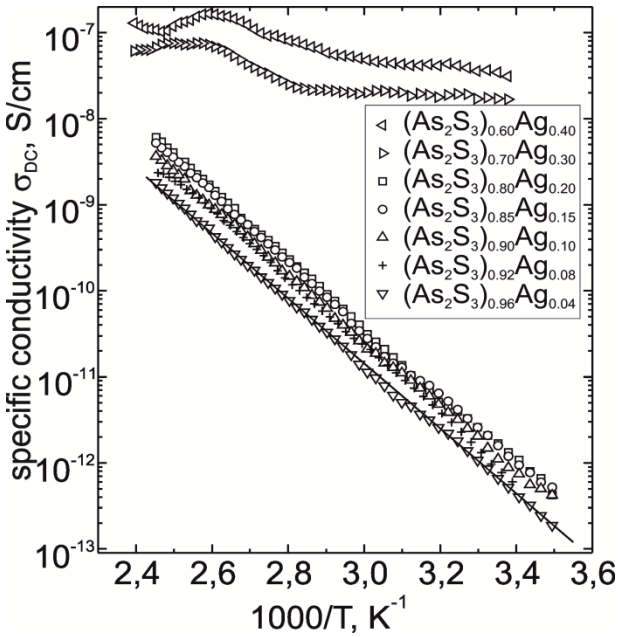

Fig. 2. Temperature dependence of DC electric conductivity σ_{DC} for as-prepared samples of $(As_2S_3)_{1-x}Ag_x$ system.

Graphic plots of the electric conductivity σ_{DC} versus inverse temperature for thermally annealed $(As_2S_3)_{1-x}Ag_x$ alloys with x = 0.08 and 0.15 are shown in Figs. 3 and 4, respectively. From the dependences measured for the $(As_2S_3)_{0.70}Ag_{0.30}$ alloy it can be seen that one-hour annealing of the amorphous samples at 523 K resulted only in a slight increase of the σ_{DC} parameter. A similar result was obtained after thermal annealing for 4 h. Based on the measurements performed for both as-prepared and annealed $(As_2S_3)_{1-x}Ag_x$ $(0.04 \le x \le 0.20)$ samples, the electric conductivity activated energy ΔE_σ was evaluated and room-temperature conductivity was estimated (Figs. 5 and 6). The ΔE_σ was shown to vary slightly with Ag content within an interval from 0.75 to 0.79 eV.

The obtained dependences and derived ΔE_σ parameter values do not provide sufficient information to judge, which of the known mechanisms of electric charge transfer is predominant in the samples under investigation. One may assume that ionic conductivity of the alloys with $x \le 0.20$ is predominantly determined by hopping conductivity of charge carriers within the existing density-of-states tails, as predicted by the Mott model [33]. According to the latter, in this case the activation energy values ΔE_σ are the difference between the Fermi level energy position and the edge of the bandgap (limited mobility gap). As a rule, in the alloys under study it roughly corresponds to half of the optical bandgap value [34].

The procedure of thermal annealing of the alloys at 523 K for 1 h resulted in an increase of the activation energy ΔE_σ by 0.2 eV (Fig. 6). More durable annealing (4 h) practically did not lease to essential increase of the activation energy value (the observed variation is within the experimental accuracy). The trend of the increase of the ΔE_σ parameter due to thermal annealing of samples

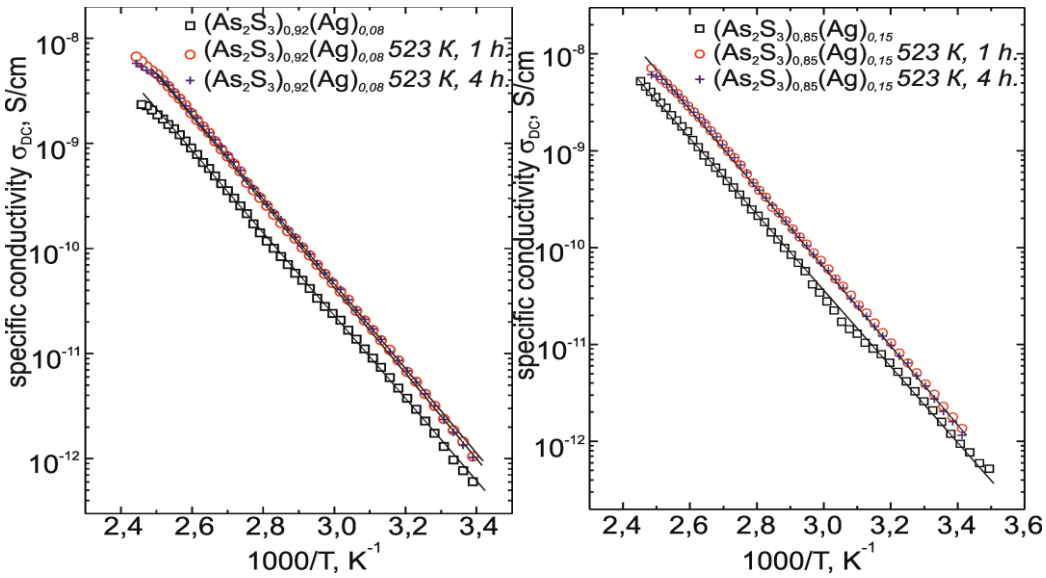

Fig. 3. Temperature dependence of DC electric conductivity σ_{DC} for the as-prepared and thermally annealed $(As_2S_3)_{1-x}Ag_x$ compounds: a – $(As_2S_3)_{0.92}Ag_{0.08}$, b – $(As_2S_3)_{0.85}Ag_{0.15}$.

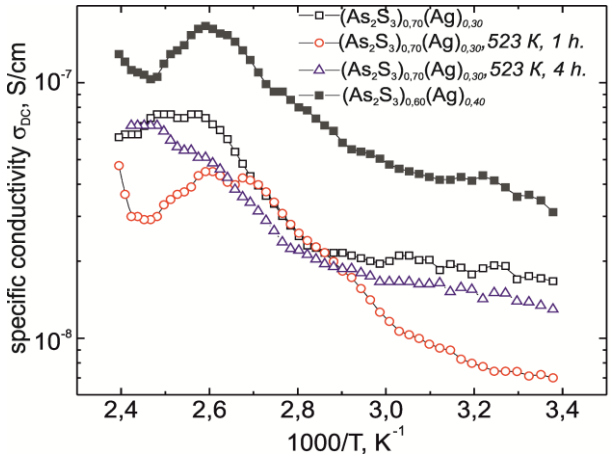

Fig. 4. Temperature dependence of DC electric conductivity σ_{DC} for the as-prepared and thermally annealed at 523 K for 1 and 4 h $(As_2S_3)_{1-x}Ag_x$ alloys (x = 0.3 and 0.4).

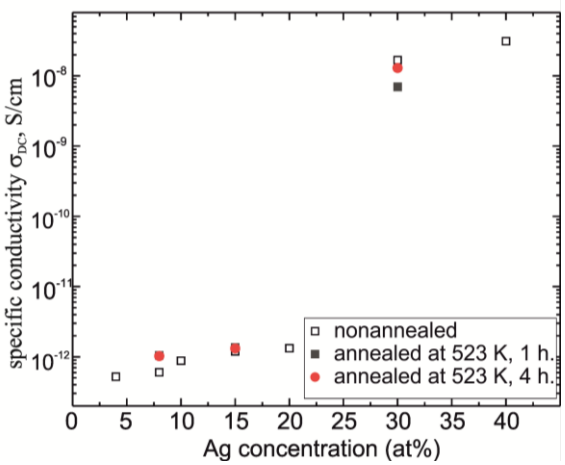

Fig. 5. Dependence of the DC electric conductivity σ_{DC} determined at room temperature, on the Ag content in $(As_2S_3)_{1-x}Ag_x$ alloys.

with relatively high Ag content observed here is somewhat different from the results obtained earlier [35] for bulk $Ag_x(As_{0.33}S_{0.67})_{1-x}$ glasses, for which the conductivity activation energy ΔE_σ decreased with silver content. From Raman scattering studies of the Ag–As–S system glasses [16, 17, 19, 29, 36] it is known that introduction of silver in small quantities leads to structural changes related to breakage of short S–S chains and bonding of S–Ag–S structural elements with pyramidal AsS_3 units. The controversy of our data and the above mentioned results can be explained by the fact that earlier [35] sulphur-enriched $Ag_x(As_{33}S_{67})_{1-x}$ glasses were studied, which are characterised by better bonding of Ag atoms with short sulphur chains. In our case, when the general content of sulphur is much lower, silver has more possibilities to bond with atoms of different structural groups [19].

Important information can be obtained from the studies of electric properties of $(As_2S_3)_{1-x}Ag_x$ alloys with high silver content ($x \geq 0.30$) using the possibilities of impedance spectroscopy in AC mode. While studying

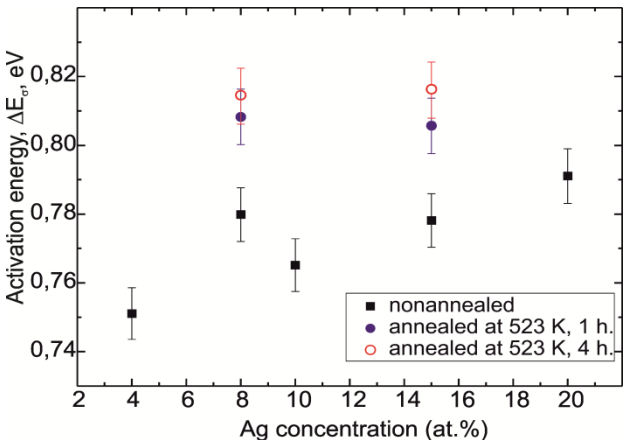

Fig. 6. Dependence of the DC conductivity activation energy ΔE_σ on the Ag content in $(As_2S_3)_{1-x}Ag_x$ alloys before and after thermal annealing.

close to Arrhenius-type $\ln(\sigma_{AC})$ versus $1/T$ dependences, we revealed the same character of variation of electric conductivity with silver content showing a distinct percolation stepwise change of the σ_{AC} value when the Ag content in the bulk alloys exceeded 20 at.% (See Fig. 7). Different slope of the linear $\ln(\sigma_{AC})$ versus $1/T$ dependences (Fig. 7) shows the presence of two components in the AC electric conductivity which depend on the character of the charge carrier thermal activation. Consequently, for different temperature intervals the derived ΔE_σ parameters are essentially different (Table 1).

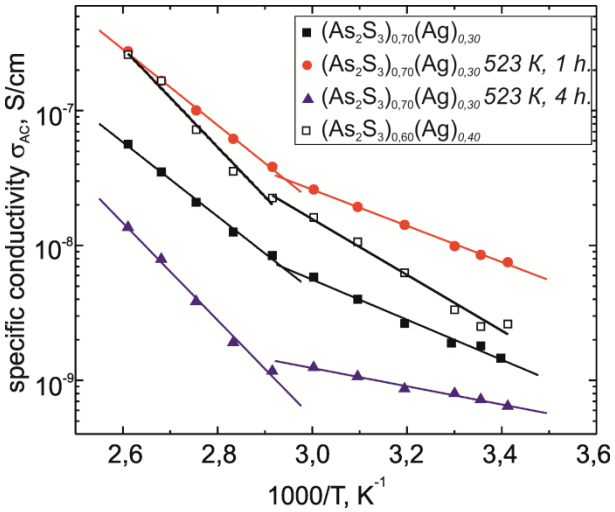

Fig. 7. Graphic plot of the type of the temperature dependence of AC electric conductivity σ_{AC} for as-prepared as well as thermally annealed at 523 K for 1 and 4 h $(As_2S_3)_{1-x}Ag_x$ alloys (x=0.30 and 0.40).

Table 1.

AC electric conductivity activation energies for $(As_2S_3)_{1-x}Ag_x$ alloys with considerable content of silver (x = 0.30 and x = 0.40).

Composition	Activation energy in the low-temperature interval, eV	Activation energy in the high-temperature interval, eV
$(As_2S_3)_{60}Ag_{40}$	0.42	0.73
$(As_2S_3)_{70}Ag_{30}$	0.29	0.54
$(As_2S_3)_{70}Ag_{30}$ annealed 1 h (523 K)	0.27	0.56
$(As_2S_3)_{70}Ag_{30}$ annealed4h (523 K)	0.13	0.71

The activation energy determined in the low-temperature interval increased with silver content (x = 0.30 and x = 0.40) from 0.29 eV to 0.42 eV. This parameter was affected by the duration of the sample annealing. Meanwhile, the activation energy ΔE_σ for the high-temperature interval increased with silver content from 0.54 eV to 0.73 eV. Thermal annealing of the sample with 30 at. % Ag resulted in a decrease of the ΔE_σ value in the low-temperature range: from 0.29 eV for the as-prepared sample to 0.27 eV and 0.13 eV for the samples annealed for 1 and 4 h, respectively. For the high-temperature range, on the contrary, this parameter was observed to increase from 0.54 eV (before annealing) to 0.56 eV (annealing for 1 h) and 0.71 eV (annealing for 4 h).

We took into account the specific feature of the AC electric conductivity for chalcogenide alloys, enriched by transition metals, when the σ_{AC} parameter at rather low frequencies is practically independent of frequency, demonstrating temperature behaviour almost identical to σ_{DC}. However, at high frequencies σ_{AC} can be affected by dispersion according to power law [37]. In the high-temperature interval, the height of the potential barrier for charge carriers expectedly decreased, hence slightly lower activation energy ΔE_σ values were obtained. Model of correlated barrier hopping proposed by Elliott [38] can be used to explain the σ_{AC}behaviour revealed in different temperature intervals. According to this model, the AC conductivity is explained by the mechanism of hopping across the energy barriers by a bipolaron, with which charge carriers overcome the potential barrier formed by spatially close D^+ and D^- charges defect centers. In our case the height of the potential barrier in the high-temperature interval correlates well with intersite distance and is due to Coulombic (interband) interaction of charged defect centers.

We assume that at lower temperatures in the AC regime hopping conductivity can be revealed, the latter being mediated by closely located localised states in the vicinity of the Fermi level, as predicted by the Mott model (variable range hopping model) [33]. Meanwhile, at higher temperatures hopping conductivity will reveal itself with participation of both localised and delocalised states adjacent to the bandgap edge [35]. Hence, ionic charge transport can be determined by their hopping from localised states close to the Fermi level to delocalised states as well as thermally determined charge carrier tunneling [39].

It was shown by energy-dispersive X-ray spectroscopy (EDX) that in bulk $(As_2S_3)_{1-x}Ag_x$ alloys with x> 0.20 a so-called phase separation of so-called liquid-liquid type is observed [19, 40], leading to the appearance of Ag-rich and Ag-poor areas (at micrometer scale). Introduction of the increasing amount of silver leads to the fragmentation of the glass local structure with increasing the relative fraction of Ag-rich areas dominating at the expense of the related reduction of the Ag-poor phase [18, 35, 41, 42]. It may be assumed that the specific features of the σ_{AC} behaviour revealed in the temperature studies with essentially different ΔE_σ parameter values are related to thermal activation of charged particles within the Ag-rich and Ag-poor areas. We take into account the fact that charge carriers are accumulated more intensely at the phase boundaries.

The disclosed features of the temperature dependences of electric conductivity of the samples with high Ag content are possibly due to various barriers and defects on the charge carrier mobility (due to the phase separation and thermally stimulated formation of new phases). The observed trend to the increase of the activation energy ΔE_σ with Ag content in the $(As_2S_3)_{1-x}Ag_x$ alloys enables us to assume that for the low-temperature range a moderate contribution to the conductivity comes from the low-Ag areas while at higher temperatures the contribution of Ag-rich areas to the

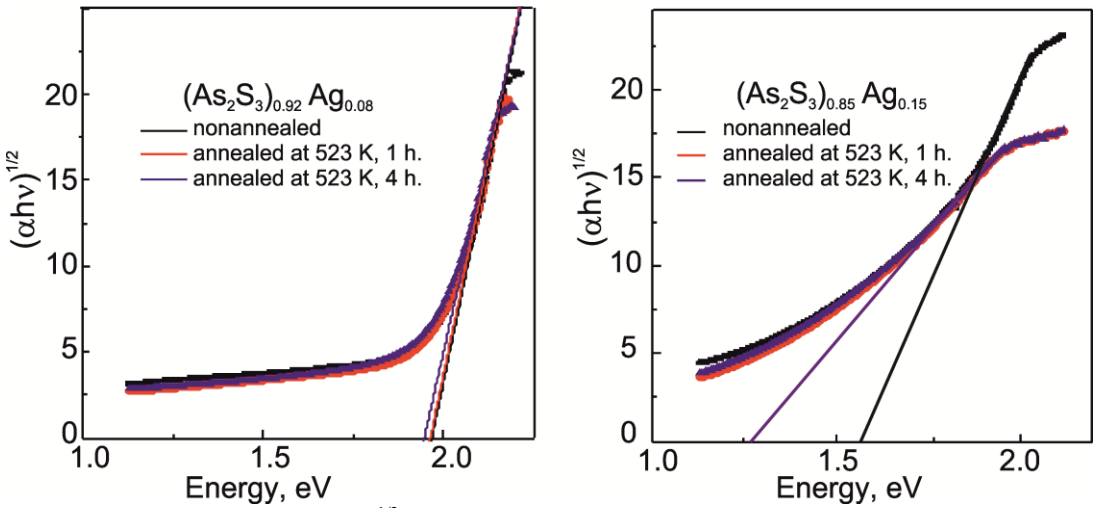

Fig. 9. Dependence of $(\alpha hv)^{1/2}$ on the photon energyhv for the as-prepared and thermally annealed $(As_2S_3)_{1-x}Ag_x$ (x =0.08 and 0.15) alloys.

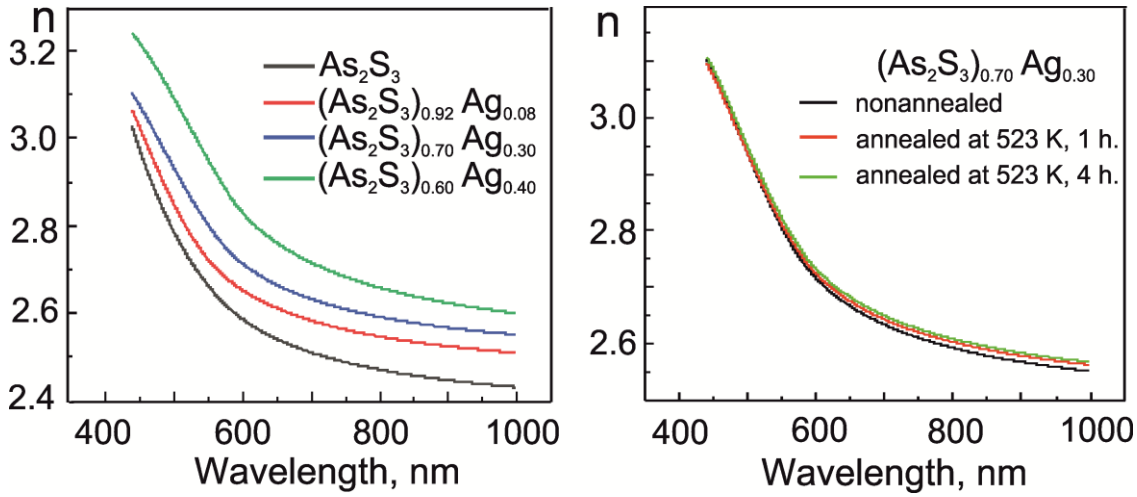

Fig. 10. Refractive index dispersion $n(\lambda)$ for the as-prepared $(As_2S_3)_{1-x}Ag_x$ alloys ($0.08 \le x \le 0.40$) and thermally annealed $(As_2S_3)_{0.70}Ag_{0.30}$ alloy.

charge transfer increases.

Study of infrared absorption spectra of the as-prepared $(As_2S_3)_{1-x}Ag_x$ alloys (Fig. 8) shows that at $x \ge 0.30$ the optical transmission coefficient essentially decreases in a broad spectral range. This is a consequence of scattering of optical waves on structural inhomogeneities in the glass, first of all due to micrometer-scale inhomogeneities in the glass, first of all due to the observed phase separation of liquid-liquid type [19, 29, 40].

For all unannealed samples with lower silver content a deep transmission minimum is observed near 14 μm. This band is due to multiphonon absorption in $(As_2S_3)_{1-x}Ag_x$ alloys (stretching vibrations of As–S bonds) and, possibly, presence of uncontrolled oxygen (As–O bond vibrations). With increasing silver content ($x \ge 0.30$) the transmission level sharply decreased what could be evidence for the increasing absorption by free charge carriers as well as formation of clusters with participation of Ag atoms (Ag–Ag separation).

In our earlier study we showed how the increasing silver concentration affects optical absorption edge in the as-prepared $(As_2S_3)_{1-x}Ag_x$ alloys in the case of

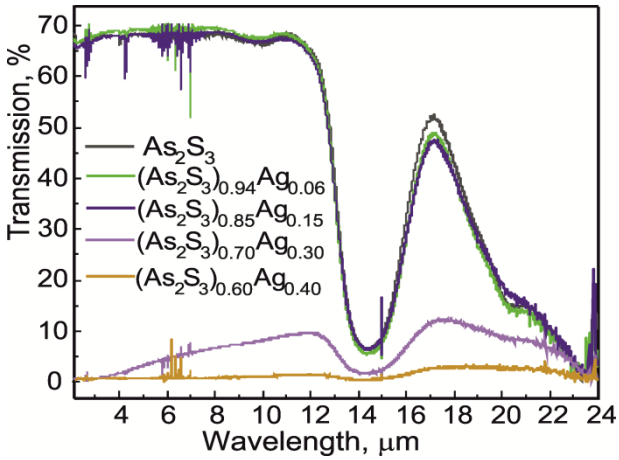

Fig. 8. Infrared optical absorption spectra of the as-prepared $(As_2S_3)_{1-x}Ag_x$ ($0 \le x \le 0.40$) alloys.

substantially lower Ag content [20]. The absorption edge shifted with x towards longer wavelengths, simultaneously the shape of the lower-energy part of the optical absorption edge "tail" changed, clearly deviating from the classical exponential shape. We explained this by silver increment-induced compositional and topological

structural disordering in glass leading to an essential increase of the density of localised states in the bandgap. In our case thermal annealing of the samples resulted in smearing and decreasing slope of the optical absorption edge in the $(As_2S_3)_{1-x}Ag_x$ alloys with $x \geq 0.15$, as can be seen from Fig. 9. In order to estimate the optical bandgap we used classical Tauc method (with certain reservations). Nevertheless, the optical bandgap E_{opt} in the $(As_2S_3)_{1-x}Ag_x$ alloys was determined as [43]

$$\alpha \cdot h\nu = B \cdot \left(h\nu - E_{opt}\right)^2 \qquad (3)$$

where α is the optical absorption coefficient, $h\nu$ is the optical photon energy, B is an alloy composition-related parameter.

Evaluation of the effect of 1-h and 4-h thermal annealing on the optical bandgap ΔE_{opt} (Fig. 9) shows that for the $(As_2S_3)_{1-x}Ag_x$ alloy with x =0.08 variation of this optical parameter can be neglected ($\Delta E_{opt} \sim 1.95$ eV) while for x = 0.15 the thermal treatment resulted in a considerable decrease of the optical bandgap ΔE_{opt} (from ~1.55 eV for the as-prepared to ~1.26 eV for the thermally annealed alloy).

Ellipsometric studies of the as-prepared and thermally annealed $(As_2S_3)_{1-x}Ag_x$ samples with high Ag content enabled us to determine their refractive index dispersion $n(\lambda)$ in the vicinity of the optical absorption edge. As can be seen from Fig. 10, increasing silver content resulted in the increase of the refractive index in the whole spectral range under study. Meanwhile, thermal annealing of the $(As_2S_3)_{0.70}Ag_{0.30}$ sample did not lead to any changes in the n (λ) dependence. Note that thermal annealing also slightly affected the spectral dependence of transmission of the $(As_2S_3)_{1-x}Ag_x$ ($x \leq 0.08$) samples in the near-infrared range.

Temperature dependence of σ_{DC} shows that in the materials under study the process of charge transfer is determined by hopping conductivity of charge carriers mediated by delocalised states within the density-of-states tails and localised states in the vicinity of the Fermi level, as predicted by the Mott model. Thermal annealing of the $(As_2S_3)_{1-x}Ag_x$ with $0.08 \leq x \leq 0.20$ for several hours resulted in an increase of both the electric conductivity σ_{DC} and the conductivity activation energy ΔE_σ (from 0.75 to 0.79 eV). For the alloys with x = 0.30 thermal annealing only slightly affected the above parameters.

The study of temperature dependence of the AC conductivity σ_{AC} in the alloys under investigation revealed presence of an additional component in the charge transfer for the as-prepared and thermally annealed $(As_2S_3)_{1-x}Ag_x$ alloys with high silver content ($x \geq 0.30$). As a result, for two different temperature intervals the obtained ΔE_σ parameter was essentially different. This is caused by the character of thermal activation of charge carriers in a medium with structural imperfection, in particular, with pronounced phase separation. Thermal annealing resulted in a somewhat decreased optical bandgap E_{opt} for the $(As_2S_3)_{1-x}Ag_x$ alloys with moderate silver content (x = 0.15).

Ellipsometric studies of the spectral dependence of the refractive index $n(\lambda)$ in the vicinity of the optical absorption edge and in the near-infrared range for the $(As_2S_3)_{1-x}Ag_x$ ($0.08 \leq x \leq 0.40$) alloys showed that increasing silver content led to an increase of $n(\lambda)$ while the thermal annealing affected this parameter only slightly.

The work was supported by the "Advanced Science in Ukraine" grant No. 2023.03/0013 by National Research Foundation of Ukraine.

Conclusions

This study presents analysis of the results of investigation of electrical and optical properties of bulk $(As_2S_3)_{1-x}Ag_x$ ($0.04 \leq x \leq 0.40$) alloys synthesised by one-temperature synthesis from a mixture of grained As_2S_3 glass and colloidal silver. Effect of thermal annealing on the alloy properties was studied. Amorphous structure of the as-prepared samples was confirmed by X-ray diffraction. Thermal annealing of $(As_2S_3)_{1-x}Ag_x$ alloys with high silver content (x = 0.30) led to the formation of Ag-containing phase inclusions, mostly in the form of crystalline smithite, in the amorphous alloy matrix.

DC electric conductivity measurement showed that increase of concentration of Ag as a structural element of the alloys under study (x > 0.20) resulted in a sharp stepwise increase of the conductivity (by four to five orders of magnitude). The increase of the DC conductivity σ_{DC} with Ag content in the alloys is most likely due to the increasing density of localised states in the energy gap.

Kryshenik V. M. – Ph. D., Senior Researcher of Department of Materials for Functional Electronics;
VoynarovychI. M. – Ph. D., Senior Researcher of Department of Materials for Functional Electronics;
Pogodin A. I. – Ph. D., Associate Professor of Department of Inorganic Chemistry;
Filep M. J. – Ph. D., Senior Researcher, Associate Professor of Department of Biology and Chemistry;
Halyan V. V. –Dr. Sci., Professor, Head of Department of Experimental Physics, Information and Educational Technologies;
Pop M. M. – Ph. D., Associate Professor of Department of Applied Physics;
Rubish V. V. – Ph. D., Senior Engineer of Department of Quantum and Plasma Electronics;
Babuka T. Y. – Ph. D., Senior Researcher of Department of Scientific Grant Activities;
Gomonnai A.V. – Dr. Sci., Professor, Head of Department of Materials for Functional Electronics.

[1] K. Tanaka, K. Shimakawa. *Amorphous Chalcogenide Semiconductors and Related Materials* (Springer, 2021); https://doi.org/10.1007/978-3-030-69598-9.

[2] B.J. Eggleton, B. Luther-Davies, K. Richardson, *Chalcogenide photonics.* Nat. Photonics, 5, 141 (2011); https://doi.org/10.1038/nphoton.2011.309.
[3] V.M. Kryshenik, Yu.M. Azhniuk, V.S. Kovtunenko, *All-optical patterning in azobenzene polymers and amorphous chalcogenides,* J. Non-Cryst. Solids, 512, 112 (2019); https://doi.org/10.1016/j.jnoncrysol.2019.02.019.
[4] L. Li, H. Lin, S. Qiao, Y. Zou, S. Danto, K. Richardson, J. D. Musgraves, N. Lu, J. Hu, *Integrated flexible chalcogenide glass photonic devices*, Nat. Photonics, 8, 643 (2014); *https://doi.org/10.1038/nphoton.2014.138.*
[5] M. Wuttig, H. Bhaskaran, T. Taubner, *Phase-change materials for non-volatile photonic applications*, Nat. Photonics, 11(8), 465 (2017); https://doi.org/10.1038/nphoton.2017.126.
[6] S.G. Sarwat, T. Moraitis, C.D. Wright, H. Bhaskaran, *Chalcogenide optomemristors for multi-factor neuromorphic computation*, Nat. Commun., 13(1), 2247 (2022); https://doi.org/10.1038/s41467-022-29870-9.
[7] T. Wagner, B. Zhang, M. Fraenkl, S. Valkova, R. Vala, T. Hrbek, *Metal-doped chalcogenides*. In: The world scientific reference of amorphous materials: Structure, Properties, Modeling and Main Applications, Structure, Properties, Modeling and Applications of Amorphous Chalcogenides, A.V. Kolobov, K. Shimakawa (Eds.) (World Scientific 2021), 1, 593 (2021); https://doi.org/10.1142/9789811215575_0018.
[8] D.M. Kavya, A.K. Sonwane, Y.N. Sudhakar, S.D. George, Y. Raviprakash, *Unveiling the role of silver-promoted phase evolution in antimony sulfide thin films for photoelectrochemical activity*, Mater. Adv., 6, 6528 (2025); https://doi.org/10.1039/D5MA00616C.
[9] S.Y. Tee, D. Ponsford, C.L. Lay, X. Wang, X. Wang, D.C. J. Neo, T. Wu, Th Warintorn, J. C. C. Yeo, G. Guan, T.-C. Lee, M.Y. Han, *Thermoelectric silver-based chalcogenides*, Adv. Sci., 9(36), 2204624 (2022); https://doi.org/10.1002/advs.202204624.
[10] A. H. Elfarash, B. Gholipour, *Reconfigurable nanoionic and photoionic material and device platforms*, Adv. Phys., X 9(1), 2338285 (2024); https://doi.org/10.1080/23746149.2024.2338285.
[11] A. Pradel, M. Ribes, *Ionic conductivity of chalcogenide glasses*, In: J.-L. Adam, X. Zhang (Eds.), Chalcogenide Glasses, (Woodhead Publishing 2014) 169 (2014); https://doi.org/10.1533/9780857093561.1.169.
[12] V. Balan, A. Piarristeguy, M. Ramonda, A. Pradel, M. Ribes, *Phase separation and ionic conductivity: an electric force microscopy investigation of silver chalcogenide glasses*, J. Optoelectron. Adv. Mater., 8, 2112 (2006).
[13] C. Holbrook, P. Chen, D.I. Novita, P. Boolchand, *Origin of conductivity threshold in the solid electrolyte glass system:* $(Ag_2S)_x(As_2S_3)_{1-x}$, IEEE Trans. Nanotechnol. 6(5), 530 (2007); https://doi.org/10.1109/TNANO.2007.905540.
[14] R. Zaiter, M. Kassem, D. Fontanari, M. Bokova, F. Cousin, T. Usuki, E. Bychkov, *Chemically-invariant percolation in silver thioarsenate glasses and two ion-transport regimes over 5 orders of magnitude in Ag content,* J. Non-Cryst. Solids, 84, 121513 (2022); https://doi.org/10.1016/j.jnoncrysol.2022.121513.
[15] S. Stehlik, J. Kolar, M. Bartos, M. Vlcek, M. Frumar, V. Zima, T. Wagner, *Conductivity in Ag–As–S (Se, Te) chalcogenide glasses,* Solid State Ion., 181(37-38), 1625 (2010); https://doi.org/10.1016/j.ssi.2010.09.016.
[16] F. Kyriazis, A. Chrissanthopoulos, V. Dracopoulos, M. Krbal, T. Wagner, M. Frumar, S.N. Yannopoulos, *Effect of silver doping on the structure and phase separation of sulfur-rich As–S glasses: Raman and SEM studies*, J. Non-Cryst. Solids, 355(37-42), 2010 (2009); https://doi.org/10.1016/j.jnoncrysol.2009.04.070.
[17] M. Ohta, M. Tsutsumi, F. Izumi, S. Ueno. *Phase separation and structural change accompanying the introduction of silver to arsenic trisulphide glass*, J. Mater. Sci., 17(8), 2431 (1982); https://doi.org/10.1007/BF00543755.
[18] M. Ohto, M. Itoh, K. Tanaka, *Optical and electrical properties of Ag–As–S glasses*, J. Appl. Phys., 77(3), 1034 (1995); https://doi.org/10.1063/1.359581.
[19] Y. Azhniuk, A. Pogodin, V. Izai, M. Filep, V. Lopushansky, V. Yukhymchuk, A.V. Gomonnai, *Phase separation and photoinduced migration of silver in* $Ag_x(As_2S_3)_{1-x}$ *glasses*, Mater. Res. Express, 12(9), 095201 (2025); https://doi.org/10.1088/2053-1591/ae0782.
[20] V.M. Kryshenik, A.I. Pogodin, M.J. Filep, I.M. Voynarovych, M.M. Pop, V.V. Rubish, A.V. Gomonnai, *Optical properties of* As_2S_3*:Ag glasses*, Phys.Chem. Sol. State, 25(4), 863 (2024); https://doi.org/10.15330/pcss.25.4.863-870.
[21] I. Kaban, P. Jóvári, T.Wágner et al., *Atomic structure of* As_2S_3*–Ag chalcogenide glasses*, J. Phys. Condens. Matter., 21(39), 395801 (2011); https://doi.org/10.1088/0953-8984/21/39/395801.
[22] M.E. Orazem, B. Tribollet, *Electrochemical impedance spectroscopy*, New Jersey, 1(906), 383 (2008); https://doi.org/10.1002/9780470381588.
[23] E. Hellner, H. Burzlaff, *Die Struktur des Smithits* $AgAsS_2$, Naturwissenschaften, 51, 35 (1964); https://doi.org/10.1007/BF00622577.
[24] T.Matsumoto, W.Nowacki, *The crystal structure of trechmannite,* $AgAsS_2$, Zeitschrift für Kristallographie, 129, 163 (1969); https://doi.org/10.1524/zkri.1969.129.1-4.163.
[25] S. Allen, *Phase transitions in proustite I. Structural studies*, Phase Transitions, 6, 1–24 (1985); https://doi.org/10.1080/01411598508219887.
[26] A.Ga, A. Pawłowski, A. Pietraszko, *Silver X-ray transfer in proustite* Ag_3AsS_3 *at high temperatures: Conductivity and single-crystal studies*, J. Sol. State Chem., 182(3), 451 (2009); https://doi.org/10.1016/j.jssc.2008.11.005.

[27] A. J. Frueh, *The crystallography of silver sulfide, Ag_2S,* Zeitschrift für Kristallographie-Crystalline Materials, 110(1-6), 136 (1958); https://doi.org/10.1524/zkri.1958.110.16.136.

[28] *T. Kawaguchi, A structural study of Ag-rich Ag–As–S glasses,* Jpn. J. Appl. Phys., 37(1R), 29 (1998); https://doi.org/10.1143/JJAP.37.2.

[29] A. Stronski, L. Revutska, A. Meshalkin, O. Paiuk, E. Achimova, A. Korchovyi, K. Shportko, O. Gudymenko, A. Prisakar, A. Gubanova, G. Triduh, *Structural properties of Ag–As–S chalcogenide glasses in phase separation region and their application in holographic grating recording*, Opt. Mater., 94, 393 (2019); https://doi.org/10.1016/j.optmat.2019.06.016.

[30] N.A. Hegab, M.A. Afifi, H.E. Atyia, A.S. Farid, *Ac conductivity and dielectric properties of amorphous $Se_{80}Te_{20-x}Ge_x$ chalcogenide glass film compositions,* J. Alloys Compd, 477(1-2), 925 (2009);https://doi.org/10.1016/j.jallcom.2008.11.129.

[31] M. Ganaie, M. Zulfequar, *Study of density of localized states in $Cd_4Se_{96-x}S_x$ (x= 0, 4, 8, 12) chalcogenide semiconductor*, J. Phys. Chem. Solids, 85, 51 (2015); https://doi.org/10.1016/j.jpcs.2015.04.013.

[32] M. A. Alvi, Z. H. Khan, *Synthesis and characterization of nanoparticle thin films of a-$(PbSe)_{100-x}Cd_x$ lead chalcogenides*, Nanoscale Res. Lett.,8(1), 148 (2013); https://doi.org/10.1186/1556-276X-8-148.

[33] N.F.Mott, E.A.Davis, *Electronic Processes in Non-CrystallineMaterials*, 2nd edn. (Oxford, Clarendon, 1979).

[34] S.R .Lukić, S.J. Skuban, F. Skuban*et al.*, *DC and AC conductivities of $(As_2S_3)_{100-x}(AsSe_{0.5}Te_{0.5l})_x$ chalcogenide glasses,* Physica B: Condens. Matter., 403(17), 2578 (2008);https://doi.org/10.1016/j.physb.2008.01.038.

[35] M. Krbal, T.Wagner, T. Srba, J. Schwarz, J. Orava, T. Kohoutek, V. Zima, L. Benes, S. O. Kasap, M. Frumar, *Properties and structure of $Ag_x(As_{0.33}S_{0.67})_{100-x}$ bulk glasses*, J. Non-Cryst. Solids, 353(13-15), 1232 (2007); https://doi.org/10.1016/j.jnoncrysol.2006.11.024.

[36] K.S. Andrikopoulos, J. Arvanitidis, V. Dracopoulos, D. Christofilos, T. Wagner, S.N. Yannopoulos, *Nanoindentation and Raman studies of phase-separated Ag–As–S glasses*, Appl. Phys. Lett., 99, 171911 (2011); https://doi.org/10.1063/1.3651494.

[37] D.Deepika, H.Singh, K.S.Rathore, N.S.Saxena. *Study of the electrical and optical properties of $Ge_{27}Se_{58}Pb_{15}$ chalcogenide glass*, J. Asian Ceram. Soc., *6*(1) 30 (2018); https://doi.org/10.1080/21870764.2018.1439612.

[38] S.R. Elliott, *A theory of a.c. conduction in chalcogenide glasses*, Philos. Mag., 36 1291 (1977); https://doi.org/10.1080/14786437708238517.

[39] A.S. Hassanien, A.A. Akl, *Electrical transport properties and Mott's parameters of chalcogenide cadmium sulphoselenide bulk glasses,* J. Non-Cryst. Solids, *432*, 471 (2016); https://doi.org/10.1016/j.jnoncrysol.2015.11.007.

[40] E.D. Zanotto, *Effect of liquid phase separation on crystal nucleation in glass-formers. Case closed,* Ceram. Int., 46(16), 24779 (2020); https://doi.org/10.1016/j.ceramint.2020.06.305.

[41] V.Zima, T.Wagner, M.Vlček *et al.*, *Electrical conductivity of $Ag_x(As_{40}Se_{60})_{100-x}$ bulk glasses,* J. Non-Cryst. Solids, 326, 159 (2003); https://doi.org/10.1016/S0022-3093(03)00398-3.

[42] Y. Miyamoto, M. Itoh, K. Tanaka, *Mobility of Ag ions in Ag–As–S glasses, Solid State Commun., 92*(11), 895 (1994);https://doi.org/10.1016/0038-1098(94)90923-7.

[43] J. Tauc, A. Menth, *States in the gap,* J. Non-Cryst. Solids, 8, 569 (1972); https://doi.org/10.1016/0022-3093(72)90194-9.

В.М. Кришеник[1], І.М. Войнарович[1], А.І. Погодін[2], М.Й.·Філеп[1,3], В.В.Галян[4], М.М. Поп[2], В.В. Рубіш[1], Т.Я. Бабука[2], О.В.Гомоннай[1]

Електрофізичні та оптичні властивості відпалених сплавів $(As_2S_3)_{1-x}Ag_x$

[1]Інститут електронної фізики НАНУ, м. Ужгород, Україна, krysheni k@gmail.com;
[2]Ужгородський національний університет, Ужгород, Україна;
[3]Закарпатський угорський університет ім. Ференца Ракоці II, Берегово, Україна;
[4]Волинський національний університет імені Лесі Українки, Луцьк, Україна

У статті представлені результати вивчення фізичних властивостей синтезованих методом гартування розплаву і також термічно відпалених сплавів $(As_2S_3)_{1-x}Ag_x$ $(0.04 \le x \le 0.40)$ залежно від рівня впровадження срібла. Виміряні в діапазоні від 293 до 413 K температурні залежності питомої електропровідності досліджуваних сплавів, зняті у режимах постійного та змінного струму, показали, що домінуючим є механізм термічно активованого перестрибування носіїв за посередництва делокалізованих станів у хвостах поблизу країв забороненої зони і локалізованих станів поблизу рівня Фермі. Енергія термічної активації іонного типу провідності сплавів, яку оцінювали на основі закону Арреніуса, зростала зі збільшенням вмісту срібла. Для об'ємних взірців $(As_2S_3)_{1-x}Ag_x$ з $x = 0.30$ і 0.40 дослідження електропровідності на змінному струмі виявили присутність двох складових у механізмі переносу зарядів, зумовлених особливостями їх неоднорідної структури. Досліджено, як збільшення вмісту Ag у сплавах $(As_2S_3)_{1-x}Ag_x$ впливає на край оптичного поглинання, ширину забороненої зони і дисперсію показника заломлення у видимому і ближньому інфрачервоному діапазонах. У термічно відпалених сплавах з високим вмістом Ag оптична ширина забороненої зони зменшується, а показник заломлення зростає.

Ключові слова: аморфні халькогеніди, електропровідність на постійному і змінному струмі, край оптичного поглинання, показник заломлення.